Direct Simulation of a Flow around an Airfoil

○ Kunio Kuwahara, Institute of Space and Astronautical Science,
Yoshinodai, Sagamihara-shi, Kanagawa 229-8510, E-mail: kuwahara@pub.isas.ac.jp
Satoko Komurasaki, College of Science and Technology, Nihon Univ.,
KandaSurugadai, Chiyoda-ku, Tokyo 101-8308, E-mail: satoko@math.cst.nihon-u.ac.jp

A flow around a subsonic airfoil is investigated computationally. Two- and three-dimensional incompressible Navier-Stokes equations are solved by finite-difference approximation without using any turbulence model. The equations are transformed to a curvilinear coordinates system of O-type topology. Also multi-directional method with third-order upwinding are employed. Computed lift coefficients agree with experimental ones very well.

1. INTRODUCTION

A flow around an airfoil is one of the most fundamental problems in aerodynamics. Many simulations have been done but some important problems still remain unsolved. Those are very unsteady flows like an impulsively started flow, flows at high angles of attack and also transition to turbulence in the boundary layer and computation using O-grid.

In this paper, those unsolved problems are attacked by solving the time-dependent incompressible Navier-Stokes equations by finite-difference approximation without using any turbulence model. Most successful simulations of this kind at high Reynolds numbers are based on the third-order upwind formulation (Kawamura and Kuwahara, 1984, Kuwahara, 1999). An approach similar in philosophy but different in method is adopted by Boris et. al. (1992). To increase the accuracy, we have developed a new finite-difference scheme named as multi-directional finite-difference method (Suito, Ishii and Kuwahara 1995). New results are presented, which will make the possibility of computational approach widen substantially.

2. COMPUTATIONAL METHOD

The governing equations are the unsteady incompressible Navier-Stokes equations and the equation of continuity as follows:

$$\mathrm{div}\boldsymbol{u} = 0 \tag{1}$$

$$\frac{\partial \boldsymbol{u}}{\partial t} + \boldsymbol{u}\cdot \mathrm{grad}\boldsymbol{u} = -\mathrm{grad}p + \frac{1}{Re}\triangle \boldsymbol{u} \tag{2}$$

where u, p, t and Re denote the velocity vector, pressure, time and the Reynolds number respectively. For high-Reynolds-number flows, time-dependent computations are required owing to the strong unsteadiness.

These equations are solved by a finite-difference method. The numerical procedure is based on the projection method. The pressure field is obtained by solving the following Poisson equation:

$$\triangle p = -\mathrm{div}(\boldsymbol{u}\cdot \mathrm{grad}\boldsymbol{u}) + \frac{D^n}{\delta t} \tag{3}$$

$$D = \mathrm{div}\boldsymbol{u} \tag{4}$$

where n is the time step and δt is the time increment. D^{n+1} is assumed to be zero, but D^n is retained as a corrective term.

A generalized coordinates system is employed, so that enough grid points can be concentrated near the body surface where the no-slip condition is imposed. In 3D case, on the side walls no-slip condition is used.

For airfoil simulation, C-grid is usually used to avoid the trailing edge singularity. To make C-grid is not easy for high angles of attack, and this is another reason of the difficulty to simulate the flow at high angles of attack. Also C-grid needs unnecessarily concentrated grid points in the near wake region beginning from the trailing edge. This makes the computation unstable. On the other hand O-grid is, in every sense, much better if the computation converges. Figure 1 shows the O-grid used here at 18 degrees attack angle.

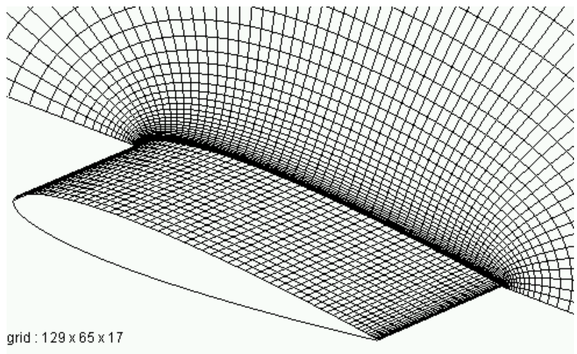

(a)

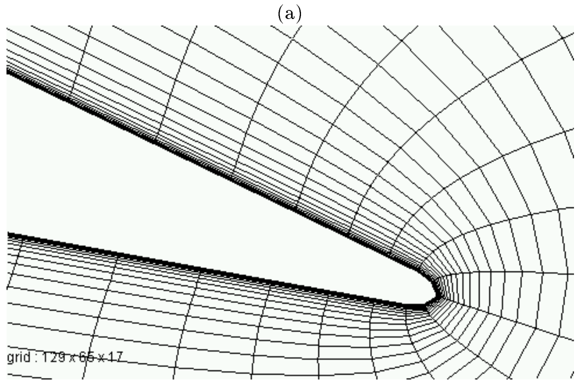

(b)

Figure 1 Computational grid

The multi-directional finite-difference method makes the computation very stable even near the trailing edge.

All the spatial derivative terms are represented by the central difference approximation except for the convection terms. For the convection terms, the third-order upwind difference is used. This is the most important point for high-Reynolds-number computations.

There is another important problem in high-order upwind schemes. That is, the accuracy decreases when the flow direction is not well parallel to one of the coordinate lines. If we use generalized coordinate system, near the boundary, the flow direction and one of the coordinate lines are almost parallel, and this problem is not serious. However, in general, flow direction is not always parallel to a coordinate line and the problem become very important.

To overcome this problem we introduced the multi-directional upwind method. This method is summarized as follows;

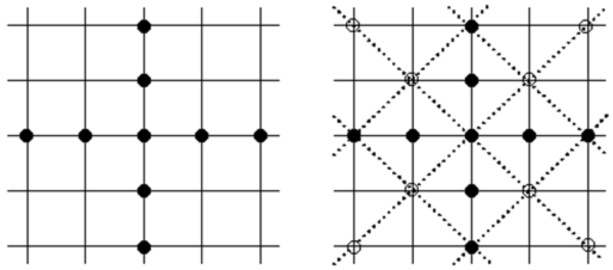

(a) system A (b) system B

Figure 2 Grid for multi-directional scheme

When structured grid points are given, the black points in Fig.2(a) are usually used to approximate the derivatives at the central point (system A).

If we introduce the other 45 degrees-rotated local grid points, the white ones in Fig.2(b), which can be used to approximate the derivatives at the central point (system B).

In order to improve a derivative value at the central point, we mix the derivative values calculated from both systems (A and B) at a proper ratio. We adopt the ratio A : B = 2/3 : 1/3. Using this ratio, for example, resulting finite-difference scheme for the Laplacian coincides with the well-known 9-points formula with forth-order accuracy. This method improves the rotational invariance of the coordinate system. Then those flows where flow direction is not parallel to the grid direction are better simulated.

For all the spatial derivatives, the multi-directional finite-difference method is used. This method has another advantage. In MAC method, usually staggered mesh is used to remove the unphysical oscillation of the pressure. This oscillations is caused by the decoupling of the computed values within the nearest two points. These values couple more tightly with the second nearest points. This decoupling becomes less if we use third-order upwind scheme because of the five-point differencing, but there remains some. However, if we use multi-directional finite-difference method, every point becomes tightly coupled and the oscillation disappears. Therefore, a non-staggered mesh system is employed where the defined positions of velocity and pressure are coincident.

For the temporal integration of the Navier-Stokes equations, the Crank-Nicolson implicit scheme is utilized. This scheme has second-order accuracy in time. These equations and the Poisson equation are iteratively solved at each time step by the successive overrelaxation (SOR) coupled with a multigrid method.

3. COMPUTATIONAL RESULTS

Two- and three-dimensional flows around airfoil at high angles of attack are computed based on the multi-directional third order upwind scheme. Fully developed 2D flow is used as an initial condition for 3D computation to save computation time. In 2D computation, it was found that agreement with experiment is perfect before the stall. However, beyond the stall angle, there exits a definite discrepancy between experiment and computation (Kuwahara and Komurasaki, 2000). Therefore, we simulated this flow using a 3D code that is developed with the same concept as the 2D code.

On the basis mentioned above, flows around an NACA0012 airfoil are simulated at angles of attack, from 0 to 24 degrees for 2D, and from 12 to 20 degrees for 3D. The number of these grid points are 128×64 (coarse grid) and 128×256 (fine grid), and 128×64×16 respectively, Reynolds number is 1,000,000.

Figure 3 shows visualized results in 2D case of the instantaneous flow field at angle attack from 14 to 20 degrees in fine grid. In this figure, the vorticity distribution, pressure contour-lines and stream lines are expressed.

In Figs. 4-7, pressure contour lines on the airfoil surface and the central plane and stream lines near the surface are shown with time history of lift coefficients at each angle attack for 3D computation.

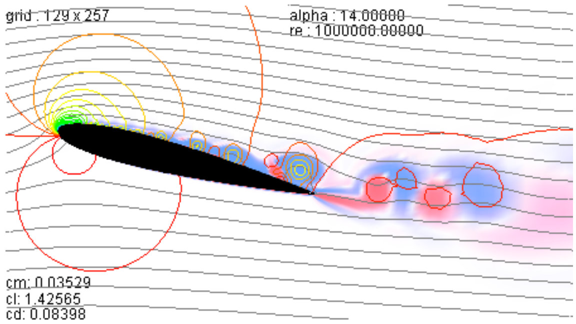

attack angle = 14 degrees

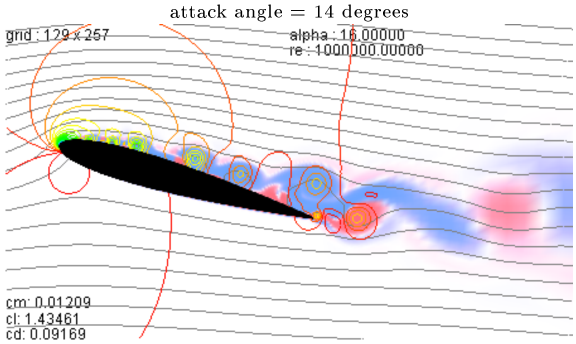

attack angle = 16 degrees

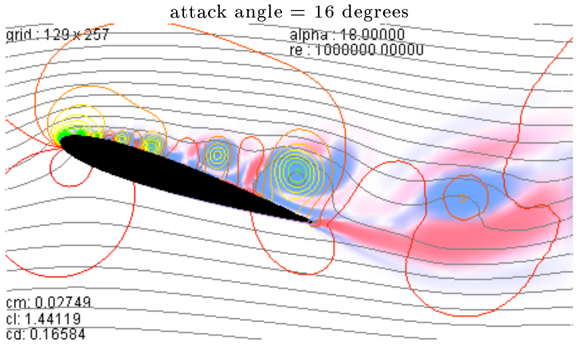

attack angle = 18 degrees

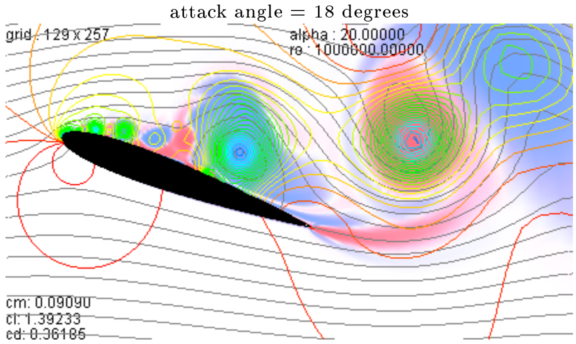

attack angle = 20 degrees

Figure 3 Instantaneous flow patterns in fine grid (128*256); stream lines, vorticity field, pressure contours

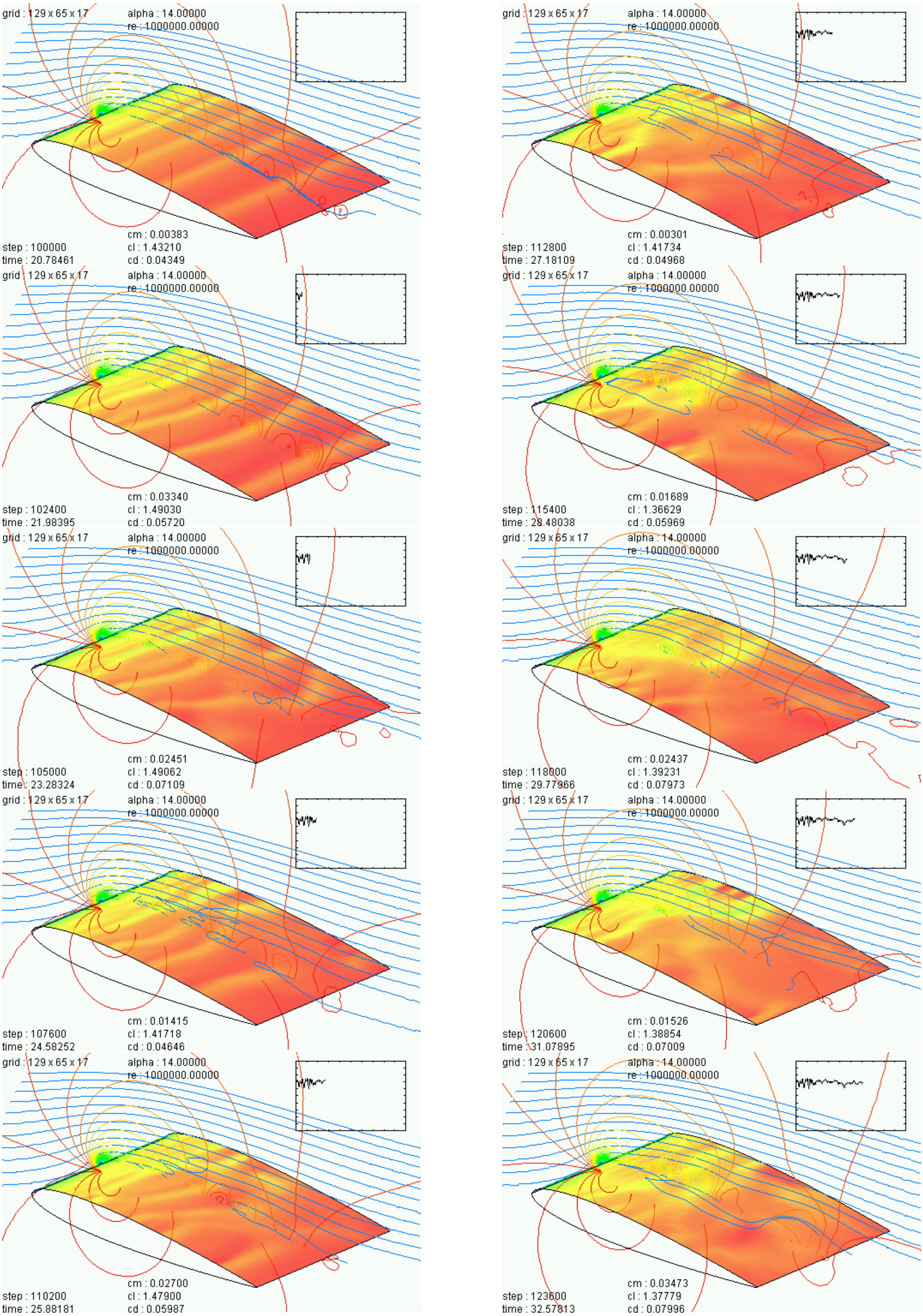

Figure 4 Time development at attack angle 14 degrees

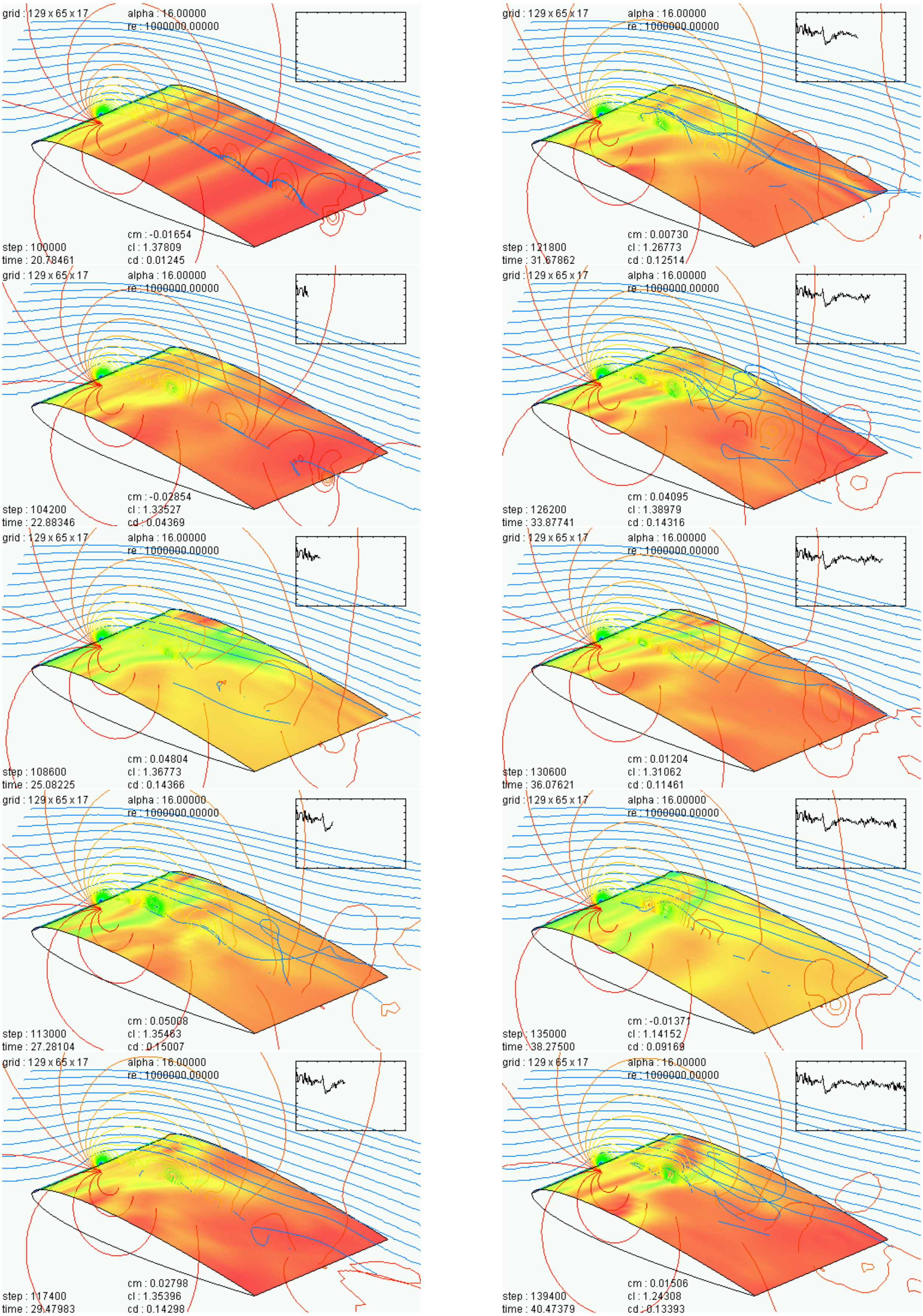

Figure 5 Time development at attack angle 16 degrees

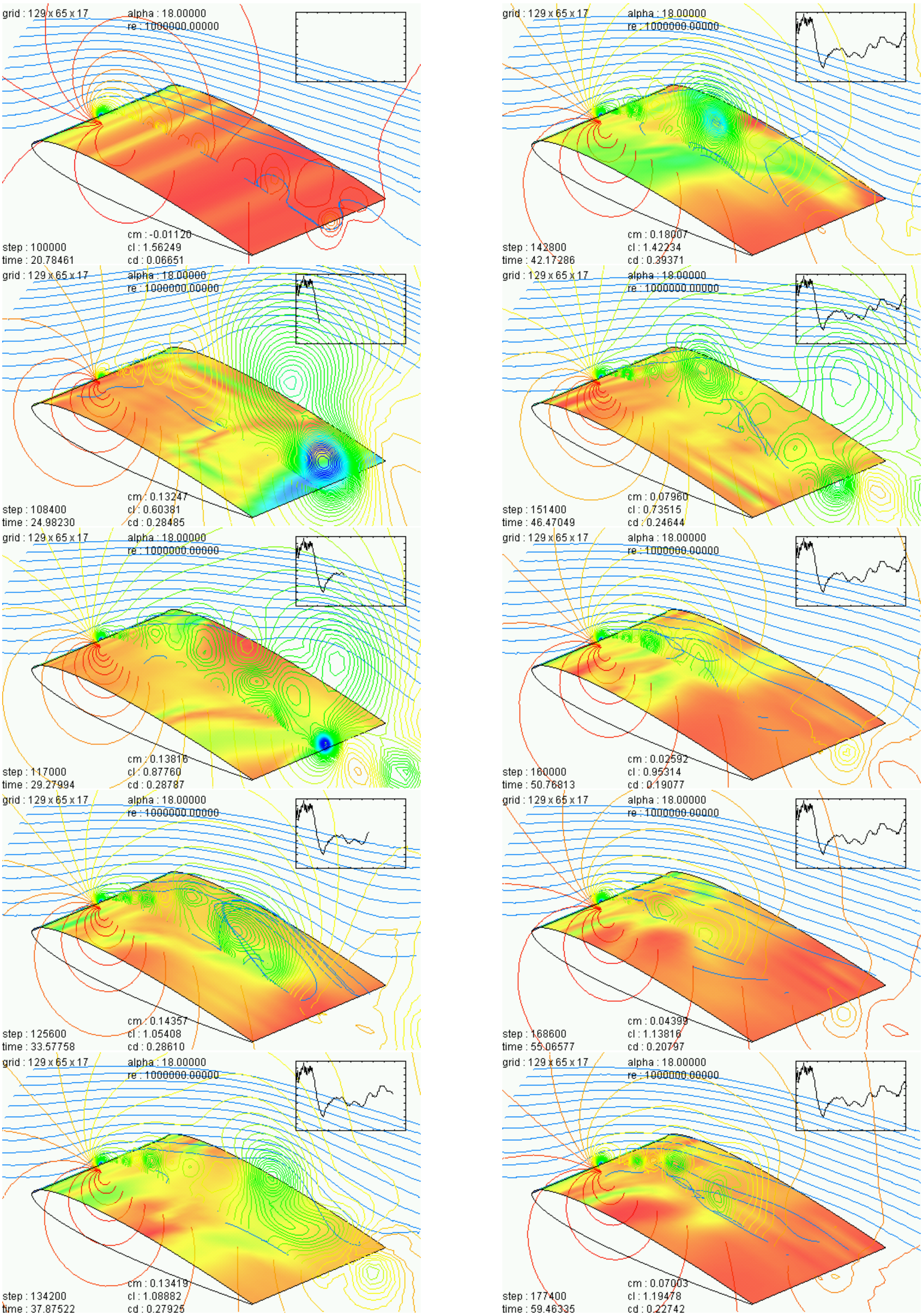

Figure 6 Time development at attack angle 18 degrees

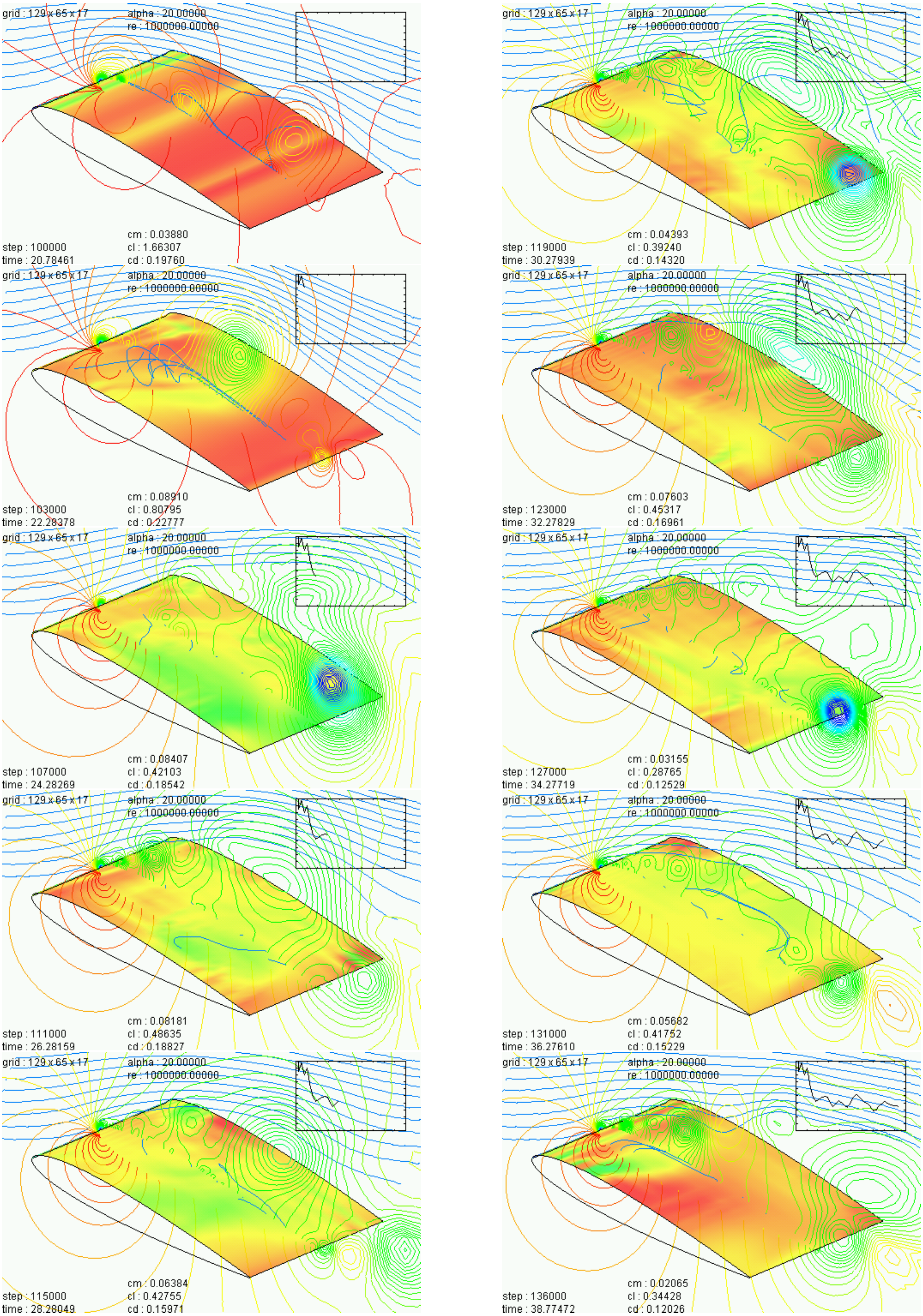

Figure 7 Time development at attack angle 20 degrees

Figure 8 shows the drag, lift and moment coefficients cd, cl, cm in 2D and 3D computations. In case of 2D computation, cl agrees perfectly well with the experimental values up to the stall angle. The lift coefficients cl become much larger than the experimental values beyond the stall angle. On the other hand, in case of 3D computation, before the stall at the attack angle 15 degrees, the lift does not change much but after the stall at attack angle 18 degrees, 3D computation quickly develops, and the lift decreases accordingly. The final results agree with the experimental ones very well (Abbott and Von Doenhoff, 1959).

Figure 9 shows drag, history of lift and moment coefficients from 2D to 3D computation at the stall angle of 18 degrees. The left side of graph shows the result of 2D computation and the other side, 3D computation with using the result of 2D computation as the starting condition.

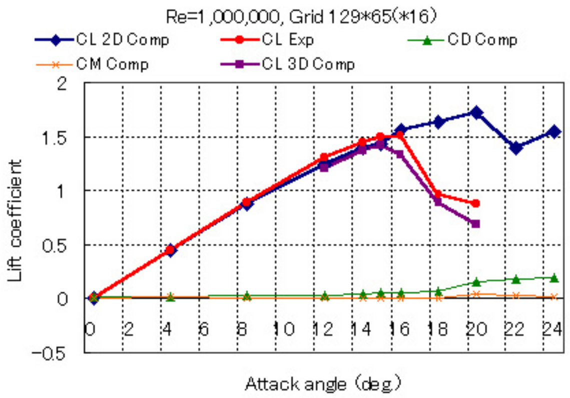

Figure 8 Drag, lift, moment coefficients

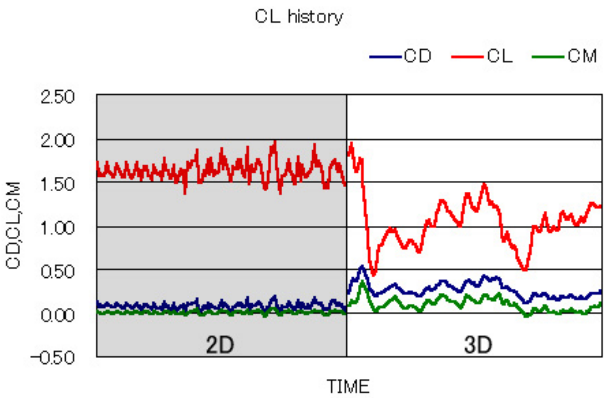

Figure 9 History of drag, lift, moment coefficients at attack angle 18 degrees

4. VISUALIZATION

The amount of computed data is becoming bigger and bigger, and without visualization system, understanding of underlying flow mechanism is very difficult. What is needed is a means of properly visualizing the computed flow field. The key points are real-time visualization and animation.

A flow simulation takes a large amount of CPU time, therefore it is desirable to visualize it while computing it. This saves a lot of time especially while debugging. This should be called real-time visualization.

Moreover, still pictures are insufficient when the flow becomes essentially unsteady as those at high Reynolds numbers, since it is impossible to understand the transient flow in total only from a set of instantaneous flow pictures. Visualization by animated graphics is a necessity in this case. Only by using such a system it becomes possible to observe the essentially unsteady flow field and to understand the fundamental flow mechanism underlying it.

The visualization software used here are Clef2D and Clef3Dvr developed by Institute of Computation Fluid Dynamics, which satisfies the above requirements (Kuzuu, Kaizaki, Kuwahara, 1997).

5. CONCLUSIONS

2D computation gives larger force coefficients beyond the stall angle. 3D computation is required for 2D flow with a large separation at high Reynolds number. Coarse 3D computation gives better results than fine 2D computation for flows with large separation.

REFERENCES

1) Kawamura, T., and Kuwahara, K., 1984, "Computation of high Reynolds number flow around a circular cylinder with surface roughness", AIAA Paper 84-0340.
2) Kuwahara, K., 1999, "Unsteady Flow Simulation and Its Visualization", AIAA Paper 99-3405
3) Boris, J.P., Grinstein, F.F., Oran, E.S., and Kolbe, R.L., 1992, "New insights into large eddy simulation", Fluid Dynamics Research 10, pp 199-228
4) Suito, H., Ishii, K., and Kuwahara, K., 1995, "Simulation of Dynamic Stall by Multi-Directional Finite-Difference Method", AIAA paper 95-2264.
5) Kuwahara, K., Komurasaki, S., 2000, "Semi-Direct Simulation of a Flow around a Subsonic Airfoil", AIAA Paper 2000-2656
6) Abbott, I. H., and Von Doenhoff, A. E., 1959, "Theory of Wing Sections", Dover Pub., pp462.
7) Kuzuu, K., and Kaizaki, H., and Kuwahara, K., 1997, "Real Time Visualization of Flow Fields Using Open GL System", AIAA Paper 97-0235.